

Dynamic response of filament winding angle on complex shaped mandrels

DOI: 10.35530/IT.071.05.1717

AHMET REFAH TORUN

ABSTRACT – REZUMAT

Dynamic response of filament winding angle on complex shaped mandrels

Aerodynamic parts such as rocket nose and heat shield related composites are mainly produced with filament winding machines. Winding angle of the reinforcement filament is the main parameter to determine the thermomechanical properties of the final composite part. The angle adjustments on the machine cause the temporary response of the filaments. This study derives an analytical method to determine the real angle of the filaments on the mandrel.

Keywords: winding angle, filament winding, composite materials, conical parts, complex shape mandrels

Răspunsul dinamic al unghiului de înfășurare al filamentelor asupra poansoanelor cu forme complexe

Piesele aerodinamice, cum ar fi vârful rachetei și materialele compozite pentru scutul termic, sunt produse în principal cu mașini pentru înfășurarea filamentelor. Unghiul de înfășurare al filamentului de armare este principalul parametru pentru a determina proprietățile termomecanice ale piesei compozite finale. Reglajele unghiului pe mașină determină răspunsul temporar al filamentelor. Acest studiu descrie o metodă analitică pentru a determina unghiul real al filamentelor de pe poanson.

Cuvinte-cheie: unghi de înfășurare, înfășurarea filamentelor, materiale compozite, piese conice, poansoane cu forme complexe

INTRODUCTION

Textile reinforced composites are used for a wide range of applications. The anisotropic nature of the composite parts extends the potential of conventional materials; however, an educated design of the layers and fiber alignment are necessary to fulfill the requirements. Filament winding is the main method to produce axially symmetrical body parts from composite materials. Winding angle of the layers is the main parameter to determine the mechanical properties. Depending on the structural design and requirements of the composite part, winding angle is changed during the production. The filament angles respond with a delay to the changing machine parameters. The aim of this study is to determine the filament angle functions analytically both for constant and changing machine settings on complex shaped mandrels.

There are many studies which analyze the effects of filament angle on the mechanical properties. Spencer and Hull have shown that both the tensile and shear strength depends on the winding angles [1]. Mistry has studied the mechanical behavior in particular bending and compression stresses of filament wound composite structures under hydrostatic pressure. The effects of winding angle were shown both experimentally and via finite elements analysis. The optimum winding angle was around 80 degrees for this coupled stress condition [2]. Filament winding on conical shapes is important for the production of aerodynamical composite structures. In the literature no study is published on the temporary response of

filament angle to the changing machine velocity. Kessels and Akkerman have developed a numerical method to determine the local angles on complex shaped braided structures [3]. Zhang et al. have analyzed the kinematical properties [4] and mechanical properties [5] of cylindrical braiding. Nishimoto et al. have developed an analytical method to predict the response of filaments on cylindrical braiding [6].

THEORETICAL APPROACH

Cylindrical mandrel

In this section, the equations of angle formations will be determined by starting with a simple cylindrical mandrel and the equations for complex shapes will be derived from this model. The mechanism of winding angle formation for filament winding on a cylindrical mandrel with constant speeds is depicted in figure 1. The tangential angle α of the filament is determined by the cylinder radius r , angular velocity of the mandrel w_0 and lateral velocity of the filament guide v_0 .

$$u_0 = r w_0 \quad (1)$$

$$\alpha = \tan^{-1} \left(\frac{r w_0}{v_0} \right) \quad (2)$$

If the angular velocity w_0 or the tangential velocity v_0 of the system is changed as a step function, it takes time for the filaments to adapt the new production conditions. This can be called as unstationary state of the system between two stationary conditions. After the new steady state is reached, the winding of filaments continues with constant angle.

The system response for the cylindrical filament winding to velocity changes can be analyzed by dividing the cross section of the cylinder with θ small angles (figure 2). For every turning of θ , the initial winding angle α_i approaches to the final winding angle α_f .

In figure 2 on the right side, the first differential step leads the filament to go to the point X_2 instead of point X_1 . In this case, the triangles Y_2X_2Z and Y_2OC are similar, therefore:

$$\frac{|OC|}{|Y_2C|} = \frac{|X_2Z|}{|ZY_2|} \quad (3)$$

If the iterations of the Y points are numbered as a_i and a_{i+1} , the equation 3 can be constructed as:

$$\frac{|OC|}{a_{i+1}} = \frac{r \cdot w_0 \cdot \Delta t}{a_i - a_{i+1} + v_f \cdot \Delta t}; \quad \Delta a = a_{i+1} - a_i \quad (4)$$

After dividing the right hand side of the equation with Δt :

$$\frac{|OC|}{r \cdot w_0} \left[-\frac{\Delta a}{\Delta t} + v_f \right] = a_{i+1}; \quad \text{where } \frac{\Delta a}{\Delta t} = \frac{da}{dt}; \quad (5)$$

$$a_{i+1} = a(t); \quad \frac{r \cdot w_0}{v_f} = \tan \alpha_f$$

$$-\frac{|OC|}{r \cdot w_0} \cdot \frac{da}{dt} = a(t) - \frac{|OC|}{\tan \alpha_f} \rightarrow \quad (6)$$

$$\rightarrow \int \frac{da}{a(t) - \frac{|OC|}{\tan \alpha_f}} = \int \frac{-r \cdot w_0 \cdot dt}{|OC|}$$

The differential equation (equation 6) can be solved by separating variables and integrating afterwards.

$$a(t) = C_0 \cdot e^{-\frac{r \cdot w_0}{|OC|} \cdot t} + \frac{|OC|}{\tan \alpha_f} \quad (7)$$

The boundary values are:

$$a(0) = \frac{|OC|}{\tan \alpha_i}; \quad a(\infty) = \frac{|OC|}{\tan \alpha_f} \quad (8)$$

After inserting boundary values into equation 7:

$$a(t) = |OC| \cdot \left[(\tan \alpha_i)^{-1} - (\tan \alpha_f)^{-1} \right] \cdot e^{-\frac{r \cdot w_0}{|OC|} \cdot t} + \frac{|OC|}{\tan \alpha_f} \quad (9)$$

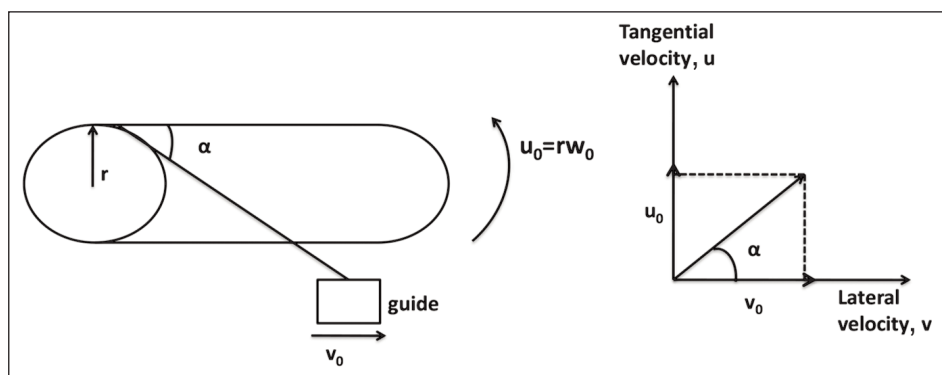


Fig. 1. Cylindrical model of filament winding with constant speeds

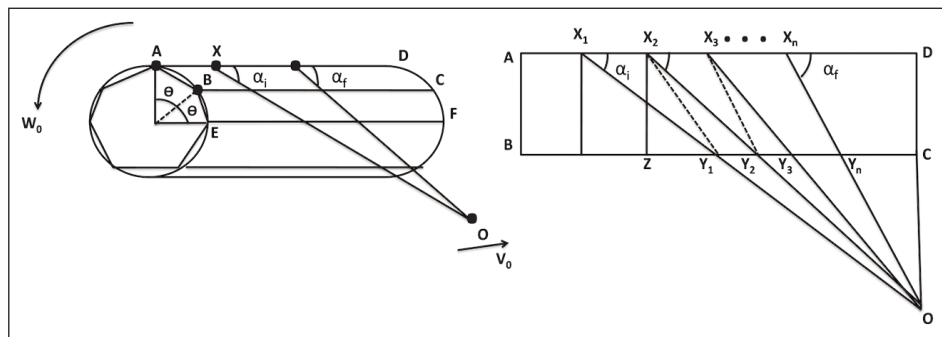


Fig. 2. Cylindrical Angle response to the velocity change

The time dependent function of $\alpha(t)$ according to the position change $a(t)$ can be written as:

$$\tan \alpha(t) = \frac{|OC|}{a(t)} \quad (10)$$

$$\alpha(t) = \tan^{-1} \left\{ \left[(\tan \alpha_i)^{-1} - (\tan \alpha_f)^{-1} \right] \cdot e^{-\frac{r \cdot w_0}{|OC|} \cdot t} + (\tan \alpha_f)^{-1} \right\}^{-1} \quad (11)$$

Conical mandrel

Filament winding on conical mandrels is used in manufacturing of aerodynamic composite structures such as rocket nose. Due to the change of mandrel radius along the length of the mandrel, the circumferential velocity of the filament changes as well. Figure 3 demonstrates the main parameters of filament winding on a conical mandrel.

The radius r of cone is changing linearly along the length, which affects the circumferential velocity. Filament guide moves laterally with the velocity of v_0 , however, the tangential lateral velocity of v_{tan} must be used to find the winding angle.

$$\cos \beta = \frac{L}{\sqrt{(R - r_0)^2 + L^2}} \quad (12)$$

$$\frac{\Delta r}{v_0 \cdot t} = \tan \beta = \frac{R - r_0}{L} \quad (13)$$

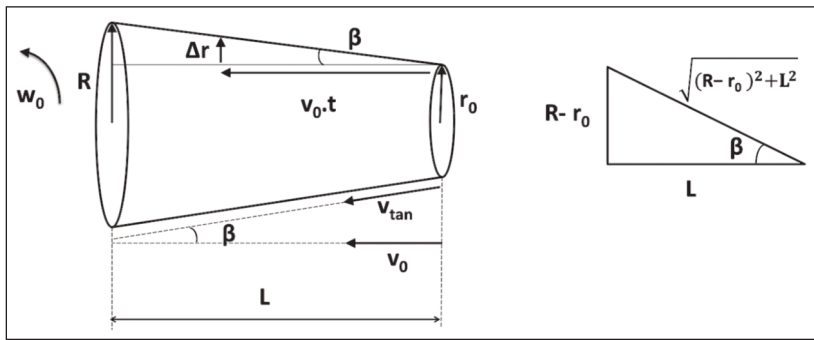


Fig. 3. Parameters on conical filament winding

$$\Delta r = v_0 \cdot t \cdot \frac{R - r_0}{L} \quad (14)$$

$$r(t) = r_0 + \Delta r = r_0 + v_0 \cdot t \cdot \frac{R - r_0}{L} \quad (15)$$

If the angular velocity w_0 and the lateral velocity v_{tan} are constant, the winding angle according to local axis on surface is:

$$\tan \alpha = \frac{r(t) \cdot w_0}{v_0} = \frac{\left[r_0 + v_0 \cdot t \cdot \frac{R - r_0}{L} \right] \cdot w_0}{v_0} \quad (16)$$

If the lateral velocity v_0 is not constant and changed as a step function to v_f , then the differential equation similar to the equation 6 defines the time dependent response of the winding angle. The difference is; radius r is not constant any more as in equation 6, instead the expression in equation 15 must be used. Tangent α_f is also changing with time, but if the angle β is small, the change can be omitted and the $\tan \alpha_f$ can be taken as constant to solve the integral.

$$-\frac{|OC|}{\left[r_0 + v_{tanf} \cdot t \cdot \frac{R - r_0}{L} \right] \cdot w_0} \cdot \frac{da}{dt} = a(t) - \frac{|OC|}{\tan \alpha_f} \quad (17)$$

$$a(t) = |OC| \cdot \left[(\tan \alpha_i)^{-1} - (\tan \alpha_f)^{-1} \right] \cdot e^{-\frac{w_0}{|OC|} \left[r_0 t + \frac{v_{tanf} \cdot (R - r_0)}{2L} \cdot t^2 \right]} + \frac{|OC|}{\tan \alpha_f} \quad (18)$$

$$\alpha(t) = \tan^{-1} \left\{ \left[(\tan \alpha_i)^{-1} - (\tan \alpha_f)^{-1} \right] \cdot e^{-\frac{w_0}{|OC|} \left[r_0 t + \frac{v_{tanf} \cdot (R - r_0)}{2L} \cdot t^2 \right]} + (\tan \alpha_f)^{-1} \right\}^{-1} \quad (19)$$

In equation v_{tanf} is the final tangential lateral velocity after the change of lateral velocity. The initial winding angle α_i and final winding angle α_f are found according to equation 16 as followed in equation 20 and 21.

$$\alpha_i(t) = \tan^{-1} \left\{ \frac{\left[r_0 + v_0 \cdot t \cdot \frac{R - r_0}{L} \right] \cdot w_0}{v_{tani}} \right\} \quad (20)$$

$$\alpha_f(t) = \tan^{-1} \left\{ \frac{\left[r_0 + v_f \cdot t \cdot \frac{R - r_0}{L} \right] \cdot w_0}{v_{tanf}} \right\} \quad (21)$$

Paraboloid mandrel

Paraboloid mandrels can be used as heat shield or aerodynamic nose part for supersonic vehicles. Such as the approach of conical mandrels is derived from the cylindrical equations, same approach can be used to derive the paraboloid equations. The differential equation (equation 6) is taken and the radius expression of paraboloid is integrated, and then the equation is solved. Figure 4 shows the main parameters of paraboloid filament winding.

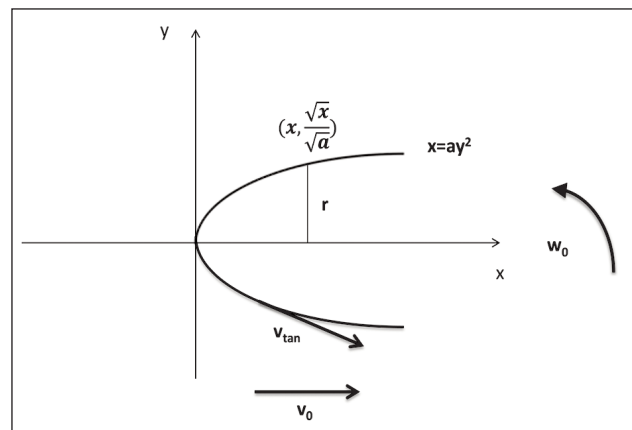


Fig. 4. Parameters on paraboloid filament winding

For the case of constant lateral guide velocity v_0 and angular velocity w_0 :

$$r = y = \frac{\sqrt{x}}{\sqrt{a}}; \quad x = v_0 \cdot t; \quad r(t) = \frac{\sqrt{v_0}}{\sqrt{a}} \cdot \sqrt{t} \quad (22)$$

$$\tan \alpha = \frac{r \cdot w_0}{v_{tan}} = \frac{\sqrt{v_0}}{\sqrt{a}} \cdot \sqrt{t} \cdot \frac{w_0}{v_{tan}} \quad (23)$$

The relation between the lateral filament guide velocity v_0 and the lateral velocity on the surface of the paraboloid v_{tan} is defined by the derivative of the parabola equation.

$$y = \frac{\sqrt{x}}{\sqrt{a}}; \quad \frac{dy}{dx} = \frac{1}{2\sqrt{ax}} = \tan \beta \quad (24)$$

$$v_{tan} = \frac{v_0}{\cos \beta} \quad (25)$$

Cos β in equation 25 can be found by drawing an imaginary right triangle by using the $\tan \beta$ expression from equation 24. The opposite edge of the right triangle is "1" and the adjacent edge is "2 \sqrt{ax} ". The equation 25 becomes:

$$v_{tan} = \frac{v_0 \cdot 2\sqrt{ax}}{\sqrt{1 + 4ax}} \quad (26)$$

The radius equation (eq. 22) is inserted into the differential equation (eq. 6).

$$-\frac{|OC|}{\sqrt{V_0}} \cdot \frac{da}{dt} = a(t) - \frac{|OC|}{\tan \alpha_f} \quad (27)$$

$$a(t) = |OC| \cdot [(\tan \alpha_i)^{-1} - (\tan \alpha_f)^{-1}] \cdot e^{-\frac{2W_0\sqrt{V_{tanf}} \cdot t^{3/2}}{3 \cdot |OC| \cdot \sqrt{a}}} + \frac{|OC|}{\tan \alpha_f} \quad (28)$$

$$\alpha(t) = \tan^{-1} \left\{ \left[(\tan \alpha_i)^{-1} - (\tan \alpha_f)^{-1} \right] \cdot e^{-\frac{2W_0\sqrt{V_{tanf}} \cdot t^{3/2}}{3 \cdot |OC| \cdot \sqrt{a}}} + (\tan \alpha_f)^{-1} \right\}^{-1} \quad (29)$$

The integration constants containing initial winding angle α_i and final winding angle α_f can be calculated via equations 30 and 31.

$$\alpha_i(t) = \tan^{-1} \left\{ \frac{\left[\frac{\sqrt{V_0}}{\sqrt{a}} \cdot \sqrt{t} \right] \cdot W_0}{V_{tani}} \right\} \quad (30)$$

$$\alpha_f(t) = \tan^{-1} \left\{ \frac{\left[\frac{\sqrt{V_f}}{\sqrt{a}} \cdot \sqrt{t} \right] \cdot W_0}{V_{tanf}} \right\} \quad (31)$$

RESULTS AND DISCUSSION

A cylindrical base model is assumed to see the time dependent response of filament winding angle to changing lateral filament guide velocity. The radius of the cylinder r is 10 cm, angular velocity is 10 rad/s, distance of filament guide to the mandrel $|OC|$ is 20 cm, initial winding angle α_i is 30° and the final winding angle α_f is 60°. According to equation 11, figure 5 shows how the filament winding angle responds to a step-wise changing of velocity.

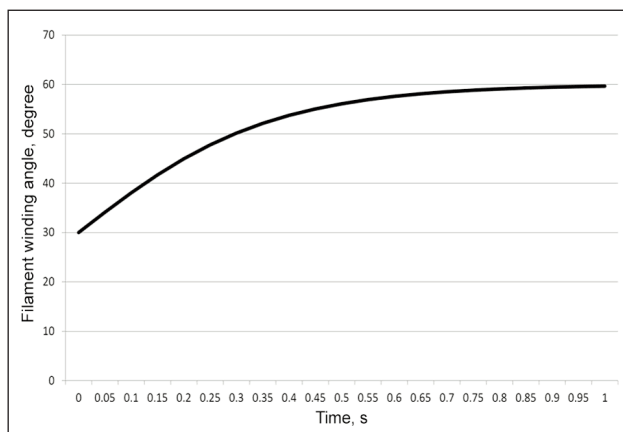


Fig. 5. Change of filament winding angle on cylindrical mandrel: 30°–60° base model

Figure 6 shows the effect of increased angular velocity from 10 rad/s of base model to 20 rad/s. As expected, the reaction of filament angle is faster and about half of the time elapses to reach the final angle

compared to the base model of figure 5. Figure 7 shows similarly the effect of increasing mandrel radius from 10 cm to 30 cm. Increasing of mandrel radius has the same accelerated reaction effect as the increasing angular velocity.

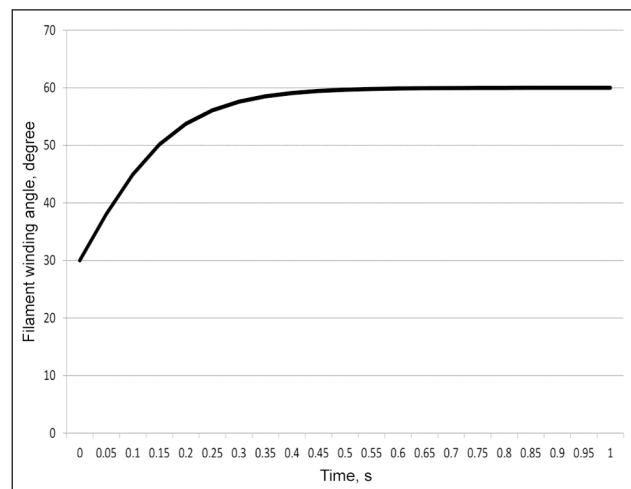


Fig. 6. Change of filament winding angle on cylindrical mandrel: 30°–60° with increased angular velocity w

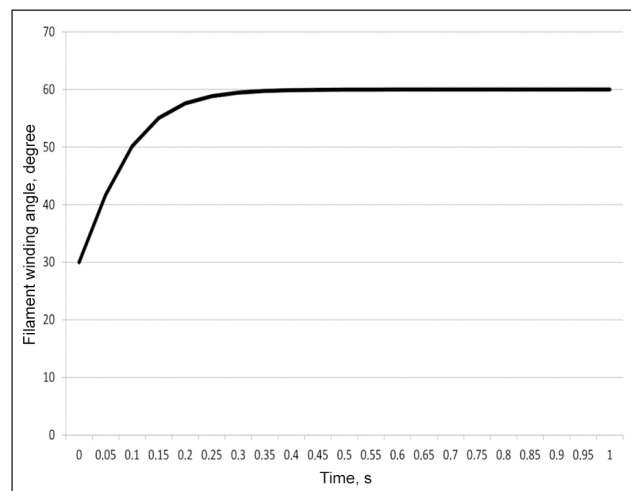


Fig. 7. Change of filament winding angle on cylindrical mandrel: 30°–60° with increased radius r

If the filament angle changes 30°–60° of base model is reversed to 60°–30°, the resulting curve is depicted in figure 8. The reaction time is a bit less compared to 30°–60° change. Changing from a higher winding angle to lower takes slightly less time than vice versa. A conical mandrel is assumed with parameters of narrow end radius 10 cm, large end radius R 20 cm, mandrel length 100 cm, angular velocity w 10 rad/s, final tangential velocity v_{tanf} 10 cm/s, distance of filament guide to the mandrel $|OC|$ 20 cm, initial winding angle α_i 30° and the final winding angle α_f 60°. Figure 9 demonstrates the angle response curve, as the conicity of the mandrel is not high, the curve looks similar to base model cylindrical mandrel, however the calculated values are slightly different due to the equation 19.

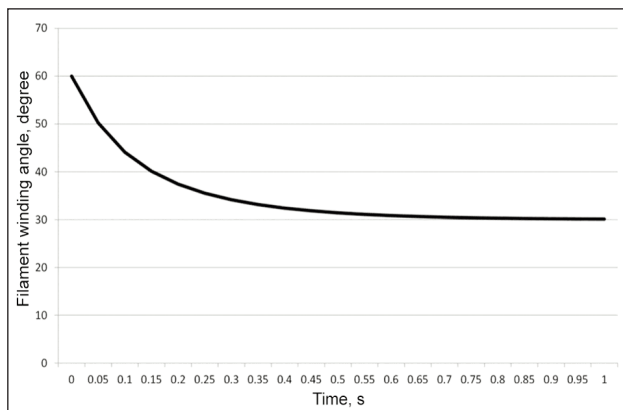


Fig. 8. Change of filament winding angle on cylindrical mandrel: 60°–30° base model

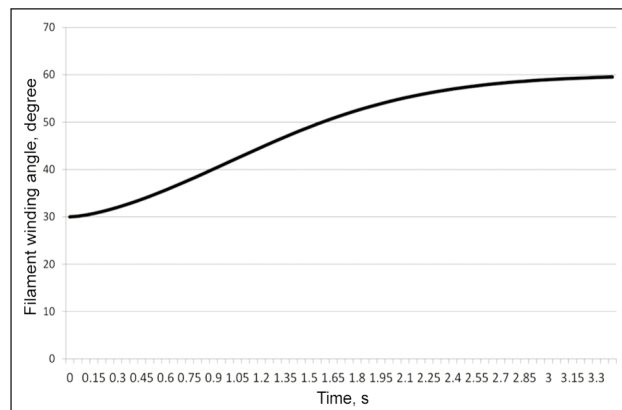


Fig. 10. Change of filament winding angle on paraboloid mandrel: 30°–60°

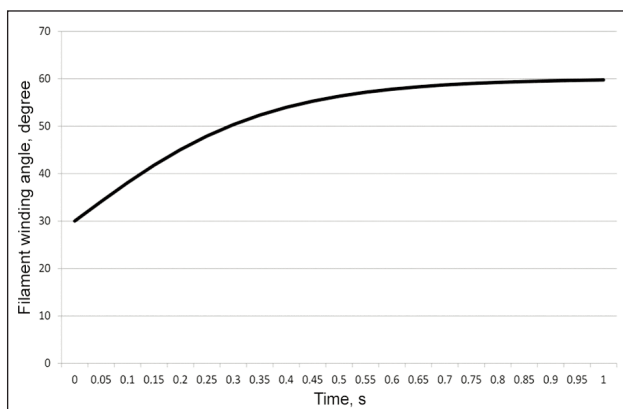


Fig. 9. Change of filament winding angle on conical mandrel: 30°–60°

Figure 10 shows the angle response curve on a paraboloid mandrel. The parameters are selected likewise to ease the comparison with previous models of figures 5–9. The angular velocity w is 10 rad/s, final tangential velocity v_{tanf} is 10 cm/s, distance of filament guide to the mandrel $|OC|$ is 20 cm, a is 2 at the curve $x = 2y^2$, initial winding angle α_i is 30° and the final winding angle α_f is 60°. According to equation 29, figure 10 shows how the filament winding angle responds to a step-wise changing of velocity. The shape of the paraboloid flattens the reaction curve of winding angle.

The cylindrical, conical and paraboloid models all have the common property of circular cross-section.

On the other hand, the elliptical mandrel yields a changing radius in the cross-section. The elliptic integral of type 2 (equation 36) does not have an analytical solution but it can only be approximated with a series expansion (equation 41). Due to the approximation, however, the time parameter “t” disappears from the equation and the responding character cannot be seen, instead if the angle is changing from 30°–60°, then the integral approaches to the mean value of 45°. Therefore, this method works only for mandrels with circular cross-sections, for other types of geometries a different approach is necessary to be developed.

CONCLUSIONS

An analytical approach is derived for the filament winding angle response on cylindrical, conical, paraboloid and elliptic cylindrical mandrels. Increasing of radius and angular velocity decreases the time elapsed to reach the final winding angle. Independent of the type of the mandrel, if the cross-section of the mandrel is circular, the method delivers applicable results. On the other hand, the method is not applicable to mandrels with cross-sections other than circular form because of the varying radius in the cross-section. A new method should be developed for mandrels with cross-sections of noncircular forms. This method provides an analytical calculation of winding angle for filament wound textile reinforced composites and structures.

REFERENCES

- [1] Spencer, B., Hull, D., *Effect of winding angle on the failure of filament wound pipe*, In: Composites, 1978, 9, 4, 263–271
- [2] Mistry, J., *Theoretical investigation into the effect of the winding angle of the fibres on the strength of filament wound GRP pipes subjected to combined external pressure and axial compression*, In: Composite Structures, 1992, 20, 2, 83–90
- [3] Kessels, J.F.A., Akkerman, R., *Prediction of the yarn trajectories on complex braided preforms*, In: Composites, Part A. Applied Science and Manufacturing, 2002, 33, 8, 1073–1081
- [4] Zhang, Q., Beale, D., Broughton, R.M., *Analysis of Circular Braiding Process, Part 1: Theoretical Investigation of Kinematics of the Circular Braiding Process*, In: Journal of Manufacturing Science and Engineering, 1999, 121, 3, 345–350

- [5] Zhang, Q., Beale, D., Broughton, R.M., Adanur, S., *Analysis of Circular Braiding Process, Part 2: Mechanics Analysis of the Circular Braiding Process and Experiment*, In: Journal of Manufacturing Science and Engineering, 1999, 121, 3, 351–359
- [6] Nishimoto, H., Ohtani, A., Nakai, A., Hamada, H., *Prediction Method for Temporal Change in Fiber Orientation on Cylindrical Braided Preforms*, In: Textile Research Journal, 2009, 80, 9, 814–821

Author:

AHMET REFAH TORUN

Adana Alparslan Türkeş Science and Technology University, Faculty of Aerospace, Aerospace Engineering,
Çatalan Caddesi 201/1, 01250, Adana, Turkey

Corresponding author:

AHMET REFAH TORUN

e-mail: artorun@atu.edu.tr